

1 **CNV-PG: a machine-learning framework for accurate copy number variation
2 predicting and genotyping**

3 **Taifu Wang^{1,2*}, Jinghua Sun^{1,2*}, Xiuqing Zhang^{1,2,3}, Wen-Jing Wang^{2#}, Qing Zhou^{2,4#}**

4 ¹BGI Education Center, University of Chinese Academy of Sciences, Shenzhen 518083, China.

5 ²BGI-Shenzhen, Shenzhen 518083, China.

6 ³Guangdong Enterprise Key Laboratory of Human Disease Genomics, Beishan Industrial Zone, Shenzhen, 518083, China.

7 ⁴Laboratory of Genomics and Molecular Biomedicine, Department of Biology, University of Copenhagen, Copenhagen, Denmark.

8 #To whom correspondence should be addressed. Email: zhouqing1@genomics.cn

9

10 **Abstract**

11 **Motivation:** Copy-number variants (CNVs) are one of the major causes of genetic disorders.
12 However, current methods for CNV calling have high false-positive rates and low concordance, and
13 a few of them can accurately genotype CNVs.

14 **Results:** Here we propose CNV-PG (CNV Predicting and Genotyping), a machine-learning
15 framework for accurately predicting and genotyping CNVs from paired-end sequencing data. CNV-
16 PG can efficiently remove false positive CNVs from existing CNV discovery algorithms, and
17 integrate CNVs from multiple CNV callers into a unified call set with high genotyping accuracy.

18 **Availability:** CNV-PG is available at <https://github.com/wonderful1/CNV-PG>

19

20 **1 Introduction**

21 Copy-number variants (CNVs) are one of the major causes of genetic disorders^[1], making accurate
22 detection of CNV essential for diagnosis of such diseases. Currently, many next-generation sequencing
23 (NGS)-based CNV detection methods have been proposed^[2]. However, most of these show high false-
24 positive rates because of the noises in the sequencing data, such as sequencing error and artificial
25 chimeric reads, and ambiguous mapping of reads cause by repeat- and duplication-rich regions^[2]. To
26 identify a set of high-confidence CNVs, a strategy that takes intersecting CNVs generated by two or
27 more algorithms is widely used. However, due to different CNV-property-dependent and library-
28 property-dependent features use by CNV detection methods, they show low concordance, causing a
29 large number of potentially true CNVs to be discarded. Besides, a few of present software can
30 accurately give the genotype of a CNV, causing a challenge for accurate detection of de novo CNVs.

31 Here, we present CNV-PG, a machine-learning framework that aims at accurately predicting and
32 genotyping true CNVs from identified results by various software. CNV-PG an open-source
33 application written in Python, including two parts (**Figure 1**): CNV predicting (CNV-P) and CNV

34 genotyping (CNV-G). For CNV-P, we trained a model on a subset of validated CNVs from 5
35 commonly used software for CNV detection separately, and obtained the corresponding classifier for
36 predicting true CNVs. For CNV-G, providing accurate genotypes for CNVs, it is compatible with
37 existing CNV detection algorithms.

38

39 **2 Methods**

40 **2.1 Data sets**

41 In CNV-P, The gold-standard CNV sets of 9 individuals (NA19238, NA19239, NA19240,
42 HG00512, HG00513, HG00514, HG00731, HG00732, HG00733) were download from Chaisson et al
43 2019^[3]. The whole genome sequences (WGS) data (~30x) of these 9 individuals were downloaded
44 from National Center for Biotechnology Information (NCBI) with accession number of SRP159517
45 (**Supplemental table. S1, S2**). For Validation sets, the sequencing data of NA12878 and HG002 were
46 also downloaded from NCBI with accession number SRP159517 and SRP047086 respectively. The
47 gold-standard CNV dataset for NA12878 was generated by three data sets: the Database of Genomic
48 Variants (<http://dgv.tcag.ca/dgv/app/home?ref=GRCh37/hg19>)^[4], the 1000 Genomes Project phaseIII
49 (https://ftp.ncbi.nih.gov/1000genomes/ftp/phase3/integrated_sv_map/)^[5], and the PacBio CNV data
50 from Pendleton, M. et al.2015^[6]. The gold-standard CNV dataset for HG002 was downloaded from
51 Zook, J. M. et al.2019^[7].

52 In CNV-G, validated genotypes and aligned bam files for 26 individuals were downloaded from
53 the 1000 Genomes Project (<https://ftp.ncbi.nih.gov/1000genomes/ftp/phase3/data/>). Sequencing data
54 of validation sample NA12878 was downloaded from NCBI with accession number SRR7782683 and
55 its genotypes were collected from Conrad. D. F. et al.2009^[8] (**Supplemental table. S1, S3**).

56

57 **2.2 Predicting**

58 A total of five commonly-used softwares (Lumpy^[8], Manta^[9], Pindel^[10], Delly^[11] and
59 breakdancer^[12]) were chosen in our study. Although these software detect CNVs based on different
60 variables, such as Pindel using the signal of split reads and Breakdancer using the information of paired
61 reads, there are consistent features for a certain CNV. We choose commonly used features in all
62 software to characterize CNVs in our training model, including size, read depth, information of paired
63 and spited read, and GC content of CNV body, as well as all these features around CNV's boundaries
64 (**Supplemental Table S1, S2**).

65

66 **2.3 Genotyping**

67 Training features were collected based on seven informative signals: depth of coverage, GC

68 content, split-reads, discordant paired-ends, CNV size ranges, CNV type, and the number of
69 chromosomes. All of these characteristics may contribute to genotyping (**Supplemental Table S1, S3**).
70

71 **3 Results**

72 **3.1 CNV-P identified a set of high-confidence CNVs with high precision and recall 73 rates**

74 To illustrate the efficiency and characteristics of the CNV-P, we used CNVs from six samples in
75 Chaisson et al 2019^[3] for training, the remaining 3 samples for evaluation (**Supplemental Table. S2**).
76 We first identified CNVs of nine samples using five frequently-used CNV callers (Lumpy^[8], Manta^[9],
77 Pindel^[10], Delly^[11] and breakdancer^[12]) respectively. For each CNV set, we removed CNVs with low
78 quality and locating on N region of genome to get the “row CNVs”. Then, we labeled CNVs as either
79 “True” or “False” based on a 50% reciprocal overlap with the gold-standard CNVs. Finally, the labeled
80 CNVs were used to train CNV-P using a Random Forest classifier and the remaining CNVs were used
81 to evaluate its performance (**Fig. 1**). we trained the CNV-P classifier on 10-fold cross-validation for
82 optimal parameter selection (**Supplemental Fig. S1**). Thus, we obtained a Random Forest classifier
83 for each CNV detection method.

84 Using the evaluation set mentioned above, each caller-specific CNV-P classifier realized
85 accurately classified the CNVs as either true or false at over 91% precision (95% for Lumpy, 93% for
86 Manta, 93% for Pindel, 92% for breakdancer, 91% for Delly) and over 87% recall rates (96% for
87 Lumpy, 95% for Manta, 93% for Pindel, 95% for breakdancer, 87% for Delly). The overall diagnostic
88 ability of each classifier, measured as the area under the Receiver Operating Characteristic (ROC)
89 curve (AUC), was 97% for Lumpy, 94% for Manta, 97% for Pindel, 93% for breakdancer, and 96%
90 for Delly (**Supplemental Fig. S2.A, B**). Additionally, we noticed that after our classification, a large
91 number of false positive CNVs were removed, and majority of the true CNVs were remained
92 (**Supplemental Fig. S2.C**). To dissect the principle of the CNV-P classifier, we assessed the relative
93 importance of each feature for corresponding classifiers. As expected, for all classifiers, read-depth
94 provided the most discriminatory power to make accurate CNV predictions (**Supplemental Fig. S3**).
95 While the second important feature inconsistent in different classifiers, it may reflect caller-specific
96 CNV signals.

97 To evaluate the robustness of each CNV-P, we trained each CNV-P on varying proportions of
98 training data (from 10% to 90% in increments of 20%). The results show a steady improvement in
99 accuracy (precise and recall rate) with an increase in the number of training data (**Supplemental Fig.**
100 **S4**). CNV-P performed well based on even 10% of training sets, showing over 90% precise rate and
101 87% recall rate. We further assessed the performance of CNV-P for different size of CNVs. We divided

102 CNVs into three sets based on their size: CNV_S (100bp to 1kb), CNV_M (1kb to 100kb), CNV_L
103 (>100kb). The overall precision of each size interval was greatly improved, comparing with the row
104 CNVs achieved by the corresponding CNV callers (**Supplemental Fig. S5**). We noticed that almost
105 all precise and recall rate in the size range of CNV_S and CNV_M were over 90%, while the theses
106 value in CNV_L was slight lower. This may be due to the insufficient number of CNV_L in our
107 training data, since they all come from healthy individuals who do not have a lot of large size of CNVs.
108 As a result, each input CNV would get a probability score predicted by CNV-P, it can be used as a
109 measurement of CNV confidence (**Supplemental Fig. S6**).

110 We also implanted two additional predictors to CNV-P, Gradient Boosting classifier (GBC) and
111 Support Vector Machine (SVM) classifier. When compared these different supervisor machine
112 learning classifiers, we found little qualitative difference between GBC and Random Forest Classifier,
113 Random Forest showed slightly better performance, and SVM was the worst performer (**Supplemental**
114 **Fig. S7**).

115 To further validate the performance of CNV-P, we implemented two independent WGS datasets
116 from NA12878 and HG002 (**Supplemental Table. S1**). In this part, each caller-specific classifier was
117 trained on data of all nine individuals mentioned above. Consistent with the above results, CNV-P
118 produced the optimal performance with AUCs of 0.94, 0.93, 0.93, 0.88 and 0.95 for Lumpy, Manta,
119 Delly, Pindel and breakdancer respectively in NA12878 (**Fig. 2A**). Most of false-positive CNVs were
120 removed with a small true positive loss (**Fig. 2B, C**). Likewise, HG002 presents the same performance
121 (**Fig. 2E-G**). Moreover, CNV-P also showed a good performance on sequencing data generate by BGI-
122 500 sequencing platform (**Supplemental Fig. S8**).

123 124 **3.2 CNV-G provide accurate genotypes of CNVs**

125 Many CNV callers have a function of genotyping CNVs, such as Manta, Delly and Lumpy with a
126 companion tool svtyper^[13]. However, some other software did not provide genotypes for CNVs. Here,
127 we also developed a machine-learning approach, named CNV-G, for genotyping a certain CNV. Model
128 selection was performed on training data using 10-fold cross-validation (**Supplemental Fig. S9**). The
129 classifier performance was independently evaluated in the NA12878.

130 To verify the performance of CNV-G, we compared it to several widely used CNV genotyping
131 tools including svtyper, Manta and Delly. We use Delly, Manta and Lumpy&svtyper to generate an
132 initial CNV set. Then, CNV-G genotyped the union from Delly, Lumpy and Manta for the validation
133 set of NA12878 whose genotypes generated by the Agilent 105K CNV genotyping array. We
134 generated a receiver operating characteristic (ROC) curves for each genotyping method. Also, we
135 implanted 3 predictors to CNV-G, Random Forest Classifier (RF), Gradient Boosting classifier (GBC)

136 and Support Vector Machine (SVM) classifier. CNV-G-RF (CNV-G based on Random Forest)
137 produced the best genotyping accuracy with AUCs of 0.95, in contrast to CNV-G-GBC (CNV-G based
138 on Gradient Boosting) and CNV-G-SVM (CNV-G based on Support Vector Machine) (**Fig. 3**).
139 Likewise, when compared to other genotyping methods, we found that CNV-P-RF produced the
140 optimal performance with AUCs of 0.95, while Manta performance resulted in an AUC of 0.91, Delly
141 and svtyper producing AUCs of 0.93 and 0.82, respectively.

142

143 **Conclusions**

144 CNV detection from WGS is error-prone because of short-read length and library-property-
145 dependent bias. Inflated false positives making a big challenge for researchers to identify clinically
146 relevant CNVs, as it is time and money consuming to validate a large amount of false positive CNVs.
147 To solve this problem, we provide CNV-PG, an effective machine-learning-based framework to
148 acquire high-quality CNVs and their genotypes. Instead of handling the shortcomings of existing
149 methods by developing another CNV caller, CNV-PG focused on creating a reliable integrative CNV
150 set from existing CNV detection software. We demonstrate that CNV-PG can identify a set of high-
151 confidence CNVs with high precision and recall rates, and the accuracy of genotypes outperform
152 present widely used CNV genotyping tools. Moreover, CNV-PG is robust to variation in the proportion
153 of training sets, CNV size and sequencing platforms, indicating the utility of CNV-PG in a variety of
154 clinical or research contexts.

155 The limitations of CNV-PG, is its dependency on a set of validated CNVs from several healthy
156 individuals. Therefore, there were not enough large size CNVs in our training data and may have
157 weaker power for large-size CNVs. Even though, our results demonstrate the utility of CNV-PG, which
158 can serve as a proof-of-principle for future studies that accumulate enough large pieces of ‘gold
159 standard’ CNVs curated from some disease samples as training data.

160 Overall, CNV-PG provides a well-performed machine-learning framework for accurately
161 predicting and genotyping CNVs, which make great sense to generate a set of high-confidence CNVs,
162 and benefit both the basic research and clinical diagnostic of genetic diseases.

163

164 **Acknowledgements**

165 The authors thank Dr. Jian Guo for constructive comments on this project and Chen Ye for data
166 download and management.

167

168 **Funding**

169 This project is supported by the National Key Research and Development Program of China

170 (No.2018YFC1004900), the National Natural Science Foundation of China (No.81300075), the
171 Science, Technology and Innovation Commission of Shenzhen Municipality under grant
172 (No.JCYJ20170412152854656, JCYJ20180703093402288).

173

174 **Conflict of interest**

175 The authors declare no conflict of interest.

176

177 **References**

1. Stankiewicz, P. and J.R. Lupski, *Structural variation in the human genome and its role in disease*. Annu Rev Med, 2010. **61**: p. 437-55.
2. Kosugi, S., et al., *Comprehensive evaluation of structural variation detection algorithms for whole genome sequencing*. Genome Biol, 2019. **20**(1): p. 117.
3. *Multi-platform discovery of haplotype-resolved structural variation in human genomes*. Nature Communications, 2019.
4. R., M.J., et al., *The Database of Genomic Variants: a curated collection of structural variation in the human genome*. Nucleic Acids Research, 2013(D1): p. D1.
5. *An integrated map of structural variation in 2,504 human genomes*. Nature. **526**(7571): p. 75-81.
6. Pendleton, M., et al., *Assembly and diploid architecture of an individual human genome via single-molecule technologies*. Nature Methods. **12**(8): p. 780-786.
7. Zook, J.M., et al., *A robust benchmark for germline structural variant detection*. bioRxiv, 2019: p. 664623.
8. Layer, R.M., et al., *LUMPY: a probabilistic framework for structural variant discovery*. Genome Biology. **15**(6): p. R84.
9. Chen, X., et al., *Manta: Rapid detection of structural variants and indels for germline and cancer sequencing applications*. Bioinformatics, 2015. **32**(8): p. 1220-1222.
10. Ye, K., et al., *Pindel: a pattern growth approach to detect break points of large deletions and medium sized insertions from paired-end short reads*. Bioinformatics. **25**(21): p. 2865-2871.
11. Rausch, T., et al., *DELLY: structural variant discovery by integrated paired-end and split-read analysis*. Bioinformatics, 2012. **28**(18): p. i333.
12. Chen, K., et al., *BreakDancer: an algorithm for high-resolution mapping of genomic structural variation*. Nat Methods, 2009. **6**(9): p. 677-81.
13. Chiang, C., et al., *SpeedSeq: ultra-fast personal genome analysis and interpretation*. Nat Methods, 2015. **12**(10): p. 966-8.

202

203

204 **FIGURE LEGENDS**

205 **Figure 1: Overview of the CNV-PG.**

206 The CNV-PG consists of two parts: CNV predicting (CNV-P) and CNV genotyping (CNV-G). In CNV-
207 P, we trained a supervised machine learning model to classify candidate CNVs as True or False. Then,
208 CNV-G was performed to accurately give the genotypes of these high-confidence CNVs.

209

210 **Figure 2: CNV-P detects high-confidence CNVs with high precision and recall rates.**

211 A, D) Receiver operating characteristic (ROC) curves of CNV-P;
212 B, E) The number of classified CNVs by CNV-P from five commonly used tools;
213 C, F) The precise and recall of CNV-P;

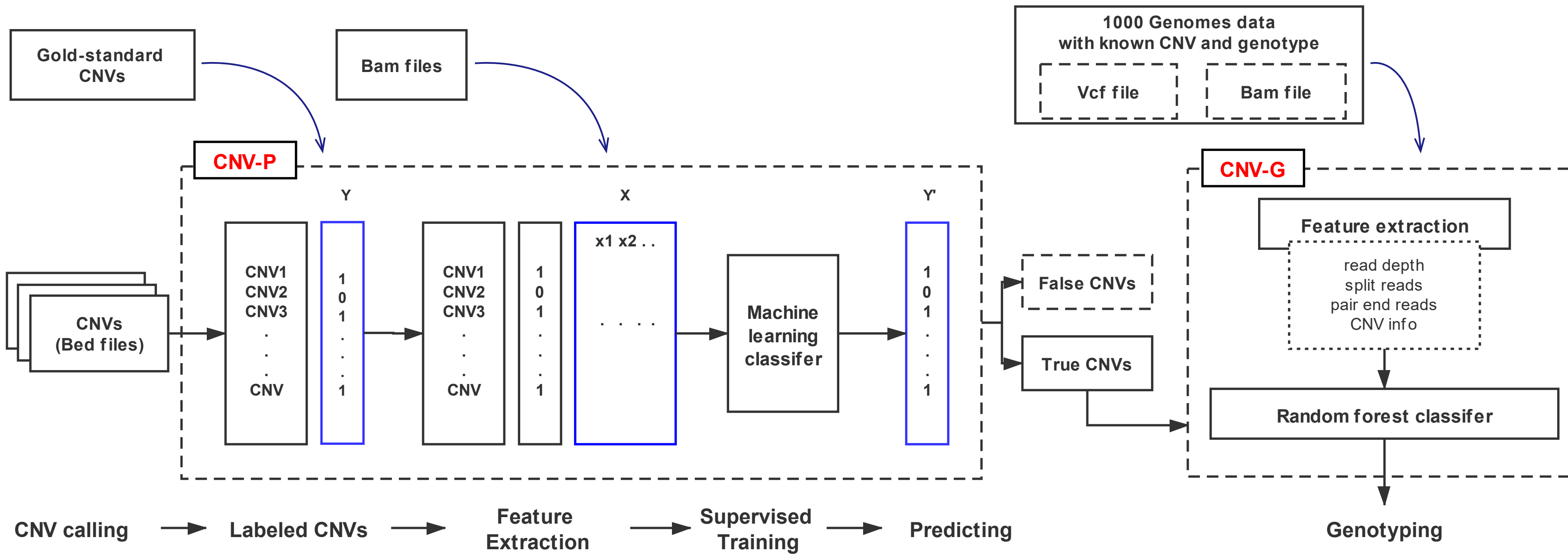
214

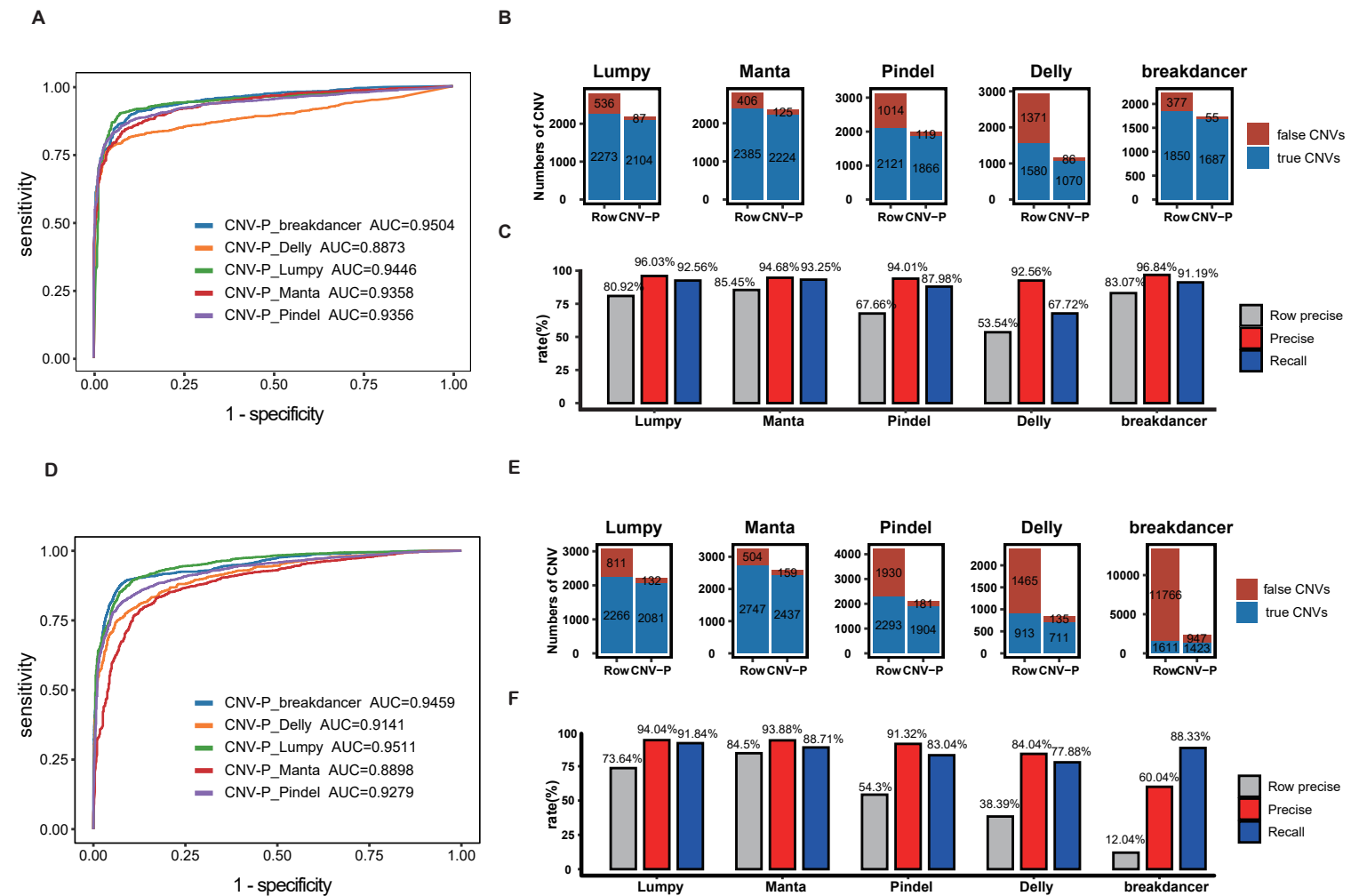
215 **Figure 3: CNV-G provides accurate genotypes of CNVs.**

216 Receiver operating characteristic (ROC) curves of genotyping for CNV-G (RF-based, GBC-based, and
217 SVM-based), Delly, Svytyper, and Manta;
218

Overview of the CNV-PG

Figure 1





CNV-G provides accurate genotypes of CNVs

